BIOCHEMISTRY
including biophysical chemistry & molecular biology

Article

pubs.acs.org/biochemistry

Structural Basis for the BRCA1 BRCT Interaction with the Proteins ATRIP and BAAT1

Xuying Liu and John A. A. Ladias*

Molecular Medicine Laboratory and Macromolecular Crystallography Unit, Department of Medicine, Harvard Medical School, Boston Massachusetts 02215, United States

ABSTRACT: The breast and ovarian cancer susceptibility protein 1 (BRCA1) plays a central role in DNA damage response (DDR). Two tandem BRCA1 C-terminal (BRCT) domains interact with several proteins that function in DDR and contain the generally accepted motif pS-X-X-F (pS denoting phosphoserine and X any amino acid), including the ATR-interacting protein (ATRIP) and the BRCA1-associated protein required for ATM activation-1 (BAAT1). The crystal structures of the BRCA1 BRCTs bound to the phosphopeptides ATRIP (235−PEACpSPQFG−243) and BAAT1 (266−VARpSPVFSS−274) were determined at 1.75 Å and 2.2 Å resolution, respectively. The pSer and Phe(+3) anchor the phosphopeptides into the BRCT binding groove, with adjacent peptide residues contributing to the interaction. In the BRCA1−ATRIP structure, Gln(+2) is accommodated through a conformational change of the BRCA1 E1698 side chain. Importantly, isothermal titration calorimetry experiments showed that the size and charge of the side chains at peptide positions +1 and +2 contribute significantly to the BRCA1 BRCT−peptide binding affinity. In particular, the Asp(+1) and Glu(+2) in the human CDC27 peptide 816−HAAEpSDEF−823 abrogate the interaction with the BRCA1 BRCTs due in large part to electrostatic repulsion between Glu(+2) and E1698, indicating a preference of these domains for specific side chains at positions +1 and +2. These results emphasize the need for a systematic assessment of the contribution of the peptide residues surrounding pSer and Phe(+3) to the binding affinity and specificity of the BRCA1 BRCTs in order to elucidate the molecular mechanisms underlying the hierarchy of target selection by these versatile domains during DDR and tumorigenesis.

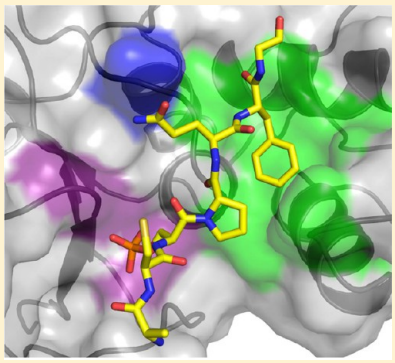

The breast and ovarian cancer susceptibility gene 1 (*BRCA1*) encodes a protein that plays a central role in genomic stability maintenance through its function in a multifaceted signaling network that involves cell cycle checkpoint control and DNA double-strand break (DSB) repair pathways, collectively referred to as the DNA damage response (DDR).[1−7] Germline mutations in the *BRCA1* gene account for the majority of familial breast and ovarian cancers.[1−4] The 1,863-residue BRCA1 protein forms a stable heterodimer with its constitutive interacting partner BARD1 that has an essential function in the maintenance of genomic integrity. The N-terminal region of BRCA1 contains a RING finger that heterodimerizes with the N-terminal BARD1 RING finger, forming an E3 ubiquitin ligase.[1−4] The C-terminal region of BRCA1 contains two tandem BRCT (BRCA1 C-terminal) domains that interact in a phosphorylation-dependent manner with a number of proteins involved in cell cycle checkpoint control and DNA repair.[8−13] Mutagenesis or deletion of the BRCT domains predisposes to cancer and suppresses the ability of BRCA1 to inhibit cancer cell growth, indicating that these domains are essential for the tumor suppressor activity of BRCA1.[1−4,11−16]

DSBs induced by ionizing radiation (IR), radiomimetic chemicals, and endogenous oxygen radicals activate the DDR signaling pathway.[6,7] The ataxia telangiectasia mutated (ATM) and ataxia telangiectasia and Rad3 related (ATR) protein kinases are among the first responders to DNA damage that initiate the DDR.[17−21] IR induces autophosphorylation of ATM at Ser1981 leading to catalytic activation of the kinase, which subsequently phosphorylates a plethora of proteins participating in DDR. ATM is recruited at the DSB sites by the Mre11−Rad50−Nbs1 (MRN) complex, where it phosphorylates histone H2AX at serine 139, which is referred to as γH2AX. The γH2AX is recognized by the BRCT domains of the mediator of DNA damage checkpoint 1 (MDC1), which facilitates recruitment of ATM and ATR to propagate γH2AX foci formation. ATR responds to DNA replication stress and is recruited to sites of stalled DNA replication forks via its obligate partner ATR-interacting protein (ATRIP), which binds to replication protein A (RPA)-coated single-stranded DNA (ssDNA). In response to DNA damage, BRCA1 is phosphorylated by ATM, ATR, and CHK2 and organizes multiple protein complexes that activate cell cycle checkpoints, DSB repair by homologous recombination (HR),[3−5] and repair of DNA interstrand cross-links independently of HR.[22] Specifically, the BRCA1 BRCT domains interact with Abraxas/CCDC98, BACH1/BRIP1, and CtIP, nucleating the assembly of three distinct complexes with specific functions, designated A, B, and C, respectively.[3,4,11] The BRCA1−A complex contains the proteins Abraxas, BRCC36, BRCC45/BRE, NBA1/MERIT40, and RAP80 and is involved in G2−M checkpoint control. The BRCA1−B complex is made up

Received: June 6, 2013
Revised: September 21, 2013
Published: September 27, 2013

dx.doi.org/10.1021/bi400714v | *Biochemistry* 2013, 52, 7618−7627

of BACH1 and TopBP1 and controls the DNA damage-induced G2 accumulation checkpoint. The BRCA1−C complex is composed of CtIP and the MRN complex and is formed in a cell cycle-dependent manner during S and G2 phases of the cell cycle. BRCA1−C is involved in DNA end resection to generate ssDNA needed for HR-mediated DNA repair. In addition to these well-studied complexes, the BRCA1 BRCTs also interact with ATRIP[23] and the BRCA1-associated protein required for ATM activation 1 (BAAT1),[24] also known as BRAT1. Phosphorylation of Ser239 in human ATRIP is recognized specifically by the BRCA1 BRCT domains, whereas a S239A substitution abrogates the BRCA1 binding to ATRIP and leads to a G2−M checkpoint defect, indicating that this interaction is essential for the ATR function in checkpoint control.[23] BAAT1 localizes to DSBs, associates with ATM, and is required for ATM autophosphorylation at Ser1981, suggesting that a coordinated assembly of BRCA1, BAAT1, and ATM is critical for DSB-induced ATM activation.[24] Importantly, mutations in the *BAAT1/BRAT1* gene have been recently associated with the lethal neonatal rigidity and multifocal seizure syndrome (RMFSL), a lethal neurologic disorder characterized by episodic jerking *in utero*, lack of psychomotor development, axial and limb rigidity, and multifocal seizures, suggesting a possible role of the BAAT1-associated DNA damage repair in neural development.[25,26] To date, the BAAT1 region that mediates the interaction with the BRCA1 BRCTs has not been reported.

A number of crystal and solution structures of the BRCA1 BRCT domains bound to phosphopeptides from BACH1,[27−29] CtIP,[30] ACC1,[31] and high-affinity peptides[32,33] showed that these domains recognize the consensus sequence pS-X-X-F (pS denoting phosphoserine and X any residue) in a two-pronged mode, with pSer and Phe(+3) inserting into two pockets, P_1 and P_2, respectively, and providing the main interactions with BRCA1 residues. In addition, these structures revealed how certain cancer-associated mutations affect the ability of the BRCTs to interact with target proteins, leading to major defects in the DDR pathway. For example, the tumor-associated mutations M1775R and M1775K abrogate the interaction of the BRCA1 BRCT repeats with their targets, and the structural analysis of these domains have provided the molecular explanation for how this is achieved at the atomic level.[27,32,34,35] However, the structural mechanisms underlying the hierarchy of target selection by the BRCA1 BRCTs, which is dictated by the sequence variation around the anchoring residues pSer and Phe(+3), are not well characterized.

Here, we present the molecular basis for the BRCA1 BRCT interaction with the proteins ATRIP and BAAT1. Isothermal titration calorimetry (ITC) experiments showed that these domains interact with the phosphopeptides PEACpSPQFG and VARpSPVFSS, corresponding to residues 235−243 and 266−274 of human ATRIP and BAAT1, respectively. The crystal structures of the BRCA1 BRCT repeats bound to the ATRIP and BAAT1 phosphopeptides reveal how these domains accommodate the side chains of Gln(+2) and Val(+2), respectively, and how residues surrounding the pSer and Phe(+3) contribute to the interaction. Unexpectedly, ITC experiments showed that the BRCA1 BRCTs do not interact with a peptide carrying Asp(+1) and Glu(+2), indicating a preference of these domains for specific side chains at positions +1 and +2. These results point to the need for a redefinition of the BRCA1 BRCT recognition motif pS-X-X-F through a precise determination of the contribution of the residues surrounding pSer and Phe(+3) to the binding affinity and specificity.

EXPERIMENTAL PROCEDURES

Protein Purification and Crystallization. The human BRCA1 BRCT protein (residues 1646−1859) was expressed in *Escherichia coli* BL21(DE3) cells as a glutathione *S*-transferase (GST) fusion and was purified as described previously.[30] Briefly, bacterial cells carrying the BRCA1(1646−1859)−pGEX-KT plasmid were grown at 37 °C, induced by the addition of 0.3 mM IPTG when Abs_{600} reached 0.6−0.8, and incubated for 15 h at 22 °C. Cells were harvested by centrifugation and resuspended in 50 mM Tris-Cl (pH 7.5), 0.5 M NaCl, 5 mM DTT, 0.2% Triton X-100, 0.5 mg/mL lysozyme, and protease inhibitor cocktail tablets (Roche). The cells were lysed by three freeze−thaw cycles, and soluble proteins were collected by centrifugation at 11000*g* at 4 °C. The supernatant was applied to a glutathione−Sepharose column (GE Healthcare), and the BRCA1(1646−1859) moiety was released with thrombin digestion and further purified by size exclusion chromatography on Superdex 75 (GE Healthcare). The purified protein was concentrated to 20 mg/mL by ultrafiltration (Millipore).

Crystallization of the BRCT−Phosphopeptide Complexes. The BRCA1 BRCT protein (20 mg/mL) was incubated with either ATRIP (PEACpSPQFG) or BAAT1 (VARpSPVFSS) peptides at a 1:1.2 molar ratio for 1 h on ice, and the resulting complexes were crystallized by the hanging-drop vapor diffusion method at 20 °C. Crystals of the BRCT−ATRIP complex were obtained in 0.2 M ammonium acetate, 0.1 M HEPES (pH 7.5), and 17−19% (w/v) PEG 3350. The crystals were cryoprotected by the addition of 25% (v/v) glycerol prior to flash-cooling in liquid nitrogen. The BRCT−BAAT1 complex was crystallized in 1 M lithium chloride, 0.1 M sodium acetate (pH 4.8), and 30% (w/v) PEG 6000, and the crystals were frozen in liquid nitrogen.

Data Collection and Processing. X-ray diffraction data sets of the BRCT−ATRIP crystals were collected at the NE-CAT 24-ID-E beamline at the Advanced Photon Source (Argonne National Laboratory, Argonne, IL). Data were indexed, scaled, and integrated using HKL2000.[36] The crystals belong to space group *P*2 with unit cell dimensions $a = 65.666$ Å, $b = 50.309$ Å, $c = 73.977$ Å, $\alpha = \gamma = 90°$, and $\beta = 116.03°$. Diffraction data sets of the BRCT−BAAT1 crystals were collected at the X25 beamline at the National Synchrotron Light Source (Brookhaven National Laboratory, Upton, NY). Data were indexed, scaled, and integrated using HKL2000. These crystals belong to space group $P3_221$ with unit cell dimensions $a = b = 65.22$ Å, $c = 91.356$ Å, $\alpha = \beta = 90°$, and $\gamma = 120°$.

Structure Determination and Refinement. The BRCT−ATRIP and BRCT−BAAT1 structures were determined by molecular replacement using PHASER[37] and the BRCA1 BRCT−CtIP structure [Protein Data Bank (PDB) entry 1Y98] with the CtIP peptide removed, as the search model. The BRCT−ATRIP structure was refined by a combination of restrained refinement, three groups of TLS refinement, and noncrystallographic symmetry in REFMAC5,[38] as implemented in the CCP4 suite.[39] Manual model correction and ligand building in COOT[40] yielded a complete model with the exception of residues 1816−1818 whose density is missing. The crystallized BRCT protein includes the vector-derived residues GS at its N terminus, which are disordered. For the BRCT−BAAT1 structure, refinement was done with rigid body refinement using REFMAC, followed by restrained refinement with REFMAC and manual model building using COOT. Water molecules were built manually. The data collection and structure

determination statistics for each complex are shown in Table 1. In the BRCT−ATRIP structure, F1798, L1800, and T1802 are located on a flexible loop and are in the disallowed region of the Ramachandran plot. In the BRCT−BAAT1 structure, E1817 located on a flexible loop was modeled as Ala because of poor electron density. The A1817 and Y1845 also fall into the disallowed region of the Ramachandran plot, although the modeled conformation of Y1845 is supported by clear electron density.

Table 1. Data Collection and Refinement Statistics

	ATRIP	BAAT1
resolution (Å)[a]	50−1.75 (1.81−1.75)	50−2.20 (2.28−2.20)
observed reflections	158123	108750
unique reflections	43821	11813
completeness (%)	99.5 (100.0)	99.5 (99.0)
R_{sym} (%)[b]	5.9 (17.8)	7.3 (53.3)
overall $\langle I/\sigma(I)\rangle$	18.2 (7.5)	31.2 (3.3)
R_{cryst} (%)[c]	15.9	19.7
R_{free} (%)[d]	20.5	26.0
bond length[e] (Å)	0.020	0.014
bond angle[e] (deg)	1.980	1.705
average B value (Å^2)	22.37	39.32
Ramachandran plot (%)		
preferred	95.9	95.7
allowed	3.3	3.3
disallowed	0.7	0.9

[a]Values in parentheses are for the highest resolution shell. [b]$R_{sym} = \Sigma|(I - \langle I\rangle)|/\Sigma(I)$, where I is the observed integrated intensity, $\langle I\rangle$ is the average integrated intensity obtained from multiple measurements, and the summation is over all observed reflections. [c]$R_{cryst} = \Sigma||F_o| - k|F_c||/\Sigma|F_o|$, where F_o and F_c are the observed and calculated structure factors, respectively. [d]R_{free} is calculated as R_{cryst} using 5% of the reflections chosen randomly and omitted from the refinement calculations. [e]Bond lengths and angles are rms deviations from ideal values.

Isothermal Titration Calorimetry. Binding constants for the BRCA1 BRCTs interaction with various phosphopeptides were measured using a VP-ITC microcalorimeter (MicroCal). Briefly, each synthetic phosphopeptide was titrated against the purified BRCA1 BRCT protein in PBS (137 mM NaCl, 2.7 mM KCl, 10 mM Na_2HPO_4, and 2 mM KH_2PO_4 at pH 7.4) at 20 °C. Each protein sample was dialyzed against PBS overnight at 4 °C, followed by further dialysis against fresh PBS for 2 h. Dilution curves of the background heat were obtained by titrating the peptides into PBS under similar conditions and were subtracted from the protein−peptide curves to determine the corrected heat for each reaction. Each experiment was repeated at least twice. Protein and peptide concentration was determined by quantitative amino acid analysis on an ABI 420A derivatizer/analyzer and an ABI 130A separation system (Applied Biosystems), where extinction coefficients were determined based on amino acid analysis. The integrated heat data were fit with a one-site binding model using the program ORIGIN 7.0 (OriginLab).

RESULTS AND DISCUSSION

BRCA1 BRCT Domains Interact with the ATRIP−pSer239 and BAAT1−pSer269 Phosphopeptides. To study the *in vitro* physical interactions of the BRCA1 BRCTs with ATRIP and BAAT1, we performed ITC experiments. The ATRIP phosphopeptide PEACpSPQFG corresponding to residues 235−243 of human ATRIP (NCBI entry NP_569055) and carrying the phospho-Ser239 interacted with

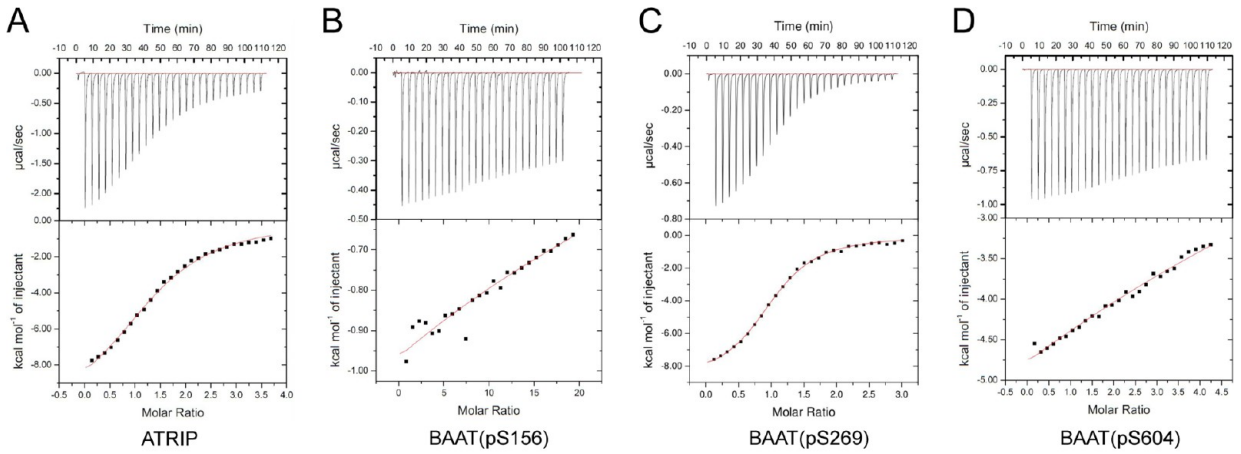

E

Peptide	Sequence	K_d (µM)	ΔG (kcal/mol)	ΔH (kcal/mol)	$-T\Delta S$ (kcal/mol)
ATRIP	PEACpSPQFG	28.2±2	−6.19±0.15	−10.4±0.2	−4.16±0.1
BAAT(pS156)	LQGDpSSLFVA	ND	ND	ND	ND
BAAT(pS269)	VARpSPVFSS	3.34±0.2	−7.34±0.1	−8.874±0.1	−1.53±0.02
BAAT(pS604)	LSVDpSEGFPR	ND	ND	ND	ND

Figure 1. Interaction of the BRCA1 BRCT domains with ATRIP and BAAT1 phosphopeptides. (A to D) Representative ITC results obtained for the BRCA1 BRCT interaction with the phosphopeptides ATRIP, BAAT(pS156), BAAT(pS269), and BAAT(pS604), respectively. For the isotherms in panels A−D, the BRCA1 BRCT concentration was 56.7 µM, 56.7 µM, 22.7 µM, and 33.3 µM, whereas the peptide concentration was 1.006 mM, 0.375 mM, 0.36 mM, and 0.683 mM, respectively. (E) Thermodynamic parameters of the BRCA1 BRCT interaction with the shown peptides. ND: not determined.

dx.doi.org/10.1021/bi400714v | *Biochemistry* 2013, 52, 7618−7627

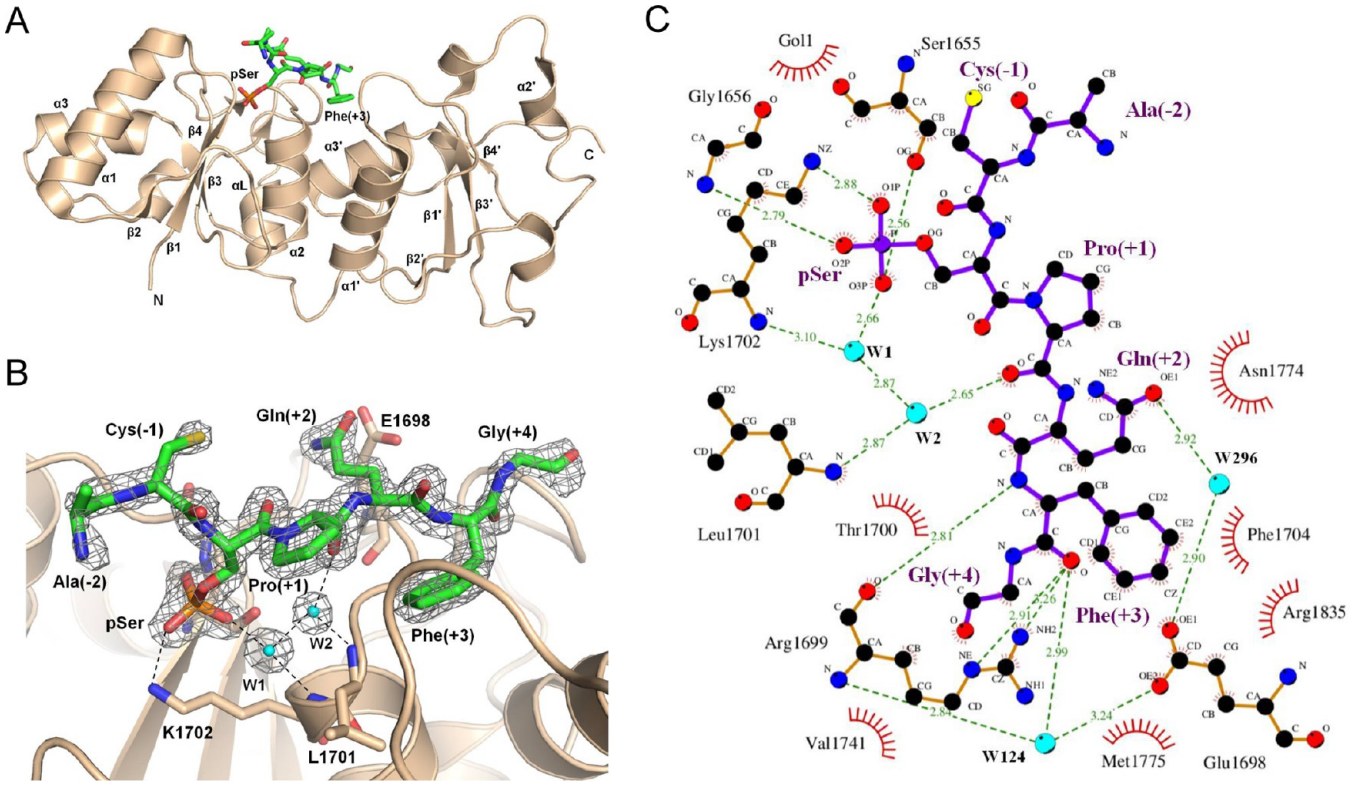

Figure 2. Structure of the BRCA1 BRCT−ATRIP complex. (A) Ribbon representation of the BRCA1 BRCTs (wheat) bound to the ATRIP peptide (green stick model). The α helices and β strands of the BRCT1 and BRCT2 repeats are labeled (those of BRCT2 are labeled with primes). The pSer and Phe(+3) are denoted. (B) A weighted $2F_o - F_c$ electron density map enveloping the peptide and two conserved water molecules (W1 and W2) calculated at 1.75 Å resolution and contoured at 1.2σ. The figure was created using PyMOL (www.pymol.org). (C) Two-dimensional representation of the interactions between BRCA1 (orange) and ATRIP (purple) residues. Water molecules (W) are shown as cyan spheres, hydrogen bonds as dashed lines, and hydrophobic interactions as arcs with radial spokes. The figure was created using LIGPLOT+.[50]

the BRCA1 BRCT domains with a K_d of 28.2 μM (Figures 1A and E), in agreement with a previous report.[23] The human BAAT1 protein sequence (NCBI entry NP_689956) contains three regions around serine residues 156, 269, and 604 that have the motif S-X-X-F, which is recognized by the BRCA1 BRCT domains when serine is phosphorylated.[2,5,14,35] To identify the BAAT1 region that interacts with the BRCA1 BRCTs, we performed ITC experiments with the phosphopeptides BAAT-(pS156), BAAT(pS269), and BAAT(pS604) having the sequences LQGDpSSLFVA, VARpSPVFSS, and LSVDpSEGFPR, corresponding to human BAAT1 residues 152−161, 266−274, and 600−609, respectively. The peptide BAAT(pS156) did not interact strongly with the BRCA1 BRCT protein, and the K_d value could not be determined accurately (Figure 1B and E). By contrast, BAAT(pS269) interacted with the BRCA1 BRCTs with a K_d of 3.3 μM (Figures 1C and E). BAAT(pS604) also failed to interact strongly with these domains (Figure 1D and E). Although the role of phospho-Ser269 in the BRCA1−BAAT1 interaction *in vivo* awaits future studies, based on the ITC results we consider that the BAAT1 region encompassing phospho-Ser269 is the major interaction site of the BRCA1 BRCTs. The inability of these domains to interact with BAAT(pS156) and BAAT(pS604) is rather unexpected because these peptides contain the pS-X-X-F recognition motif. Taken together, these results provide evidence that certain amino acids surrounding the anchoring residues pSer and Phe(+3) reduce the binding affinity for the BRCA1 BRCT domains.

Structural Determinants of the BRCA1 BRCTs Binding to ATRIP. To elucidate the structural basis for the BRCA1 BRCT interaction with the ATRIP phosphopeptide, we determined the crystal structure of this complex at 1.75 Å resolution. As described previously, the BRCA1(1646−1859) region forms two tandem domains, BRCT1 and BRCT2, each consisting of four parallel β strands (β1 to β4) flanked by two α helices (α1 and α3) on one side and a single α helix (α2) on the other (Figure 2A). A head-to-tail packing of BRCT1 and BRCT2 buries a large hydrophobic interface and creates a surface groove with two pockets, P_1 and P_2. The ATRIP peptide inserts into this groove with phospho-Ser239 and Phe242 (+3) entering the P_1 and P_2 pockets, respectively, and forming the main interactions with the BRCT1 and BRCT2 modules (Figure 2B and C). The present structure is consistent with previous biochemical and functional studies on the importance of phospho-Ser239 for the BRCA1−ATRIP association.[23] The O^{1P} atom of pSer forms a hydrogen bond with the N^{ζ} of K1702, O^{2P} hydrogen bonds with the amide nitrogen of G1656, and O^{3P} forms hydrogen bonds directly with the O^{γ} of S1655 and through a water-mediated interaction with the amide nitrogen of K1702 (Figure 2C). The phenyl ring of Phe(+3) is inserted into the hydrophobic pocket P_2 formed by R1699, L1701, F1704, N1774, M1775, R1835, and L1839. The amide nitrogen of Phe(+3) hydrogen bonds with the carbonyl oxygen of R1699. The carbonyl oxygen of Phe(+3) hydrogen bonds with the N^{ε} and $N^{\eta 2}$ of R1699, and through a water-mediated interaction with the amide nitrogen of R1699 and the $O^{\varepsilon 2}$ of E1698. The carbonyl oxygen of Pro(+1) participates in a water-mediated hydrogen bond network with the O^{3P} of pSer and the amide nitrogens of L1701 and K1702 (Figure 2C). The $O^{\varepsilon 1}$ atom of Gln(+2) forms a hydrogen bond

dx.doi.org/10.1021/bi400714v | *Biochemistry* 2013, 52, 7618−7627

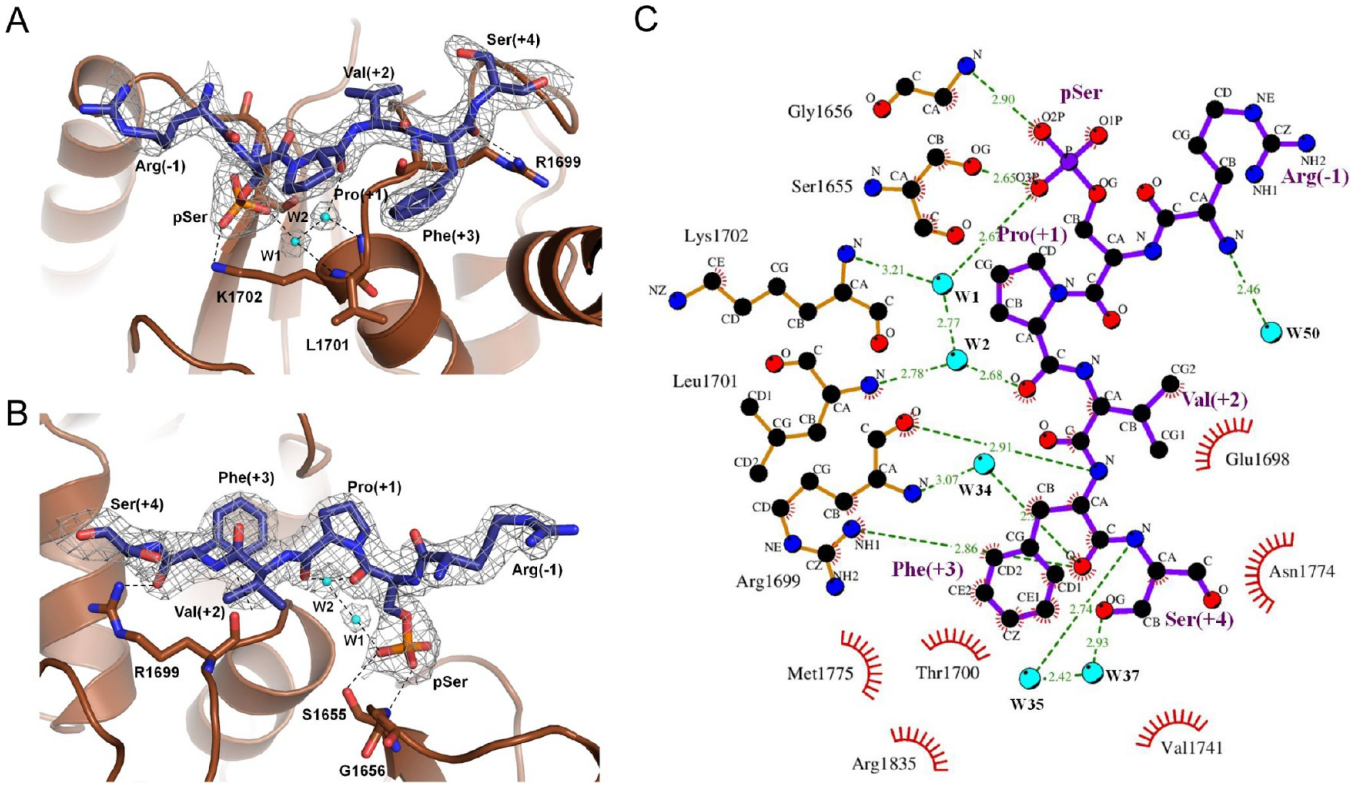

Figure 3. BAAT1 recognition by the BRCA1 BRCT domains. (A and B) Ribbon representation of the BRCA1 BRCTs (brown) bound to the BAAT1 peptide (blue stick model) with a weighted $2F_o - F_c$ electron density map enveloping the peptide and two water molecules (W1 and W2) calculated at 2.2 Å resolution and contoured at 1.2σ. In B, the model is rotated by 180° along the vertical axis. (C) Two-dimensional representation of the interactions between BRCA1 (orange) and BAAT1 (purple) residues. The hydrogen bond between the pSer O^{1P} and the N^{ζ} of K1702 is not shown. The figure was created using LIGPLOT^{+}.

with the $O^{\epsilon 1}$ of E1698 through a water-mediated interaction. Additional van der Waals contacts between ATRIP residues Pro(+1), Gln(+2), Phe(+3), and Gly(+4) contribute to the interaction, whereas Cys(−1), Ala(−2), Glu(−3), and Pro(−4) do not seem to interact with BRCA1 residues (Figure 2C).

Structural Basis for BAAT1 Recognition by the BRCA1 BRCTs. To determine the molecular mechanisms underlying the BRCA1 BRCT interaction with the BAAT(pS269) phosphopeptide (henceforth referred to as BAAT1 since it is the main interaction site of BRCA1), we solved the crystal structure of this complex at 2.2 Å resolution. As expected, the phospho-Ser269 and Phe272 (+3) form the main interactions with the BRCT domains (Figure 3A and B). The O^{1P} atom of pSer forms a hydrogen bond with the N^{ζ} of K1702, the O^{2P} of pSer hydrogen bonds with the amide nitrogen of G1656, and the O^{3P} forms hydrogen bonds with the O^{γ} of S1655 and the amide nitrogen of K1702 through a water-mediated interaction (Figure 3A–C). The phenyl ring of Phe(+3) is inserted into the P_2 pocket with the carbonyl oxygen of Phe(+3) hydrogen bonding with the $N^{\eta 1}$ of R1699 and through a water-mediated interaction with the amide nitrogen of R1699. The amide nitrogen of Phe(+3) hydrogen bonds with the carbonyl oxygen of R1699. To a lesser degree, the BAAT1 residues Pro(+1), Val(+2), and Ser(+4) also contribute to the interaction through van der Waals contacts and water-mediated hydrogen bonds, whereas Arg(−1), Ala(−2), Val(−3), and Ser(+5) do not participate in interactions with BRCA1 residues (Figure 3C).

Structural Comparison of the BRCT–ATRIP and BRCT–BAAT1 Complexes. Superposition of the BRCA1 BRCTs bound to ATRIP and BAAT1 phosphopeptides shows that the BRCT domains and the backbones of five residues of the two peptides (positions 0 to +4) are superimposed well with a root-mean-square (rms) deviation of 0.097 Å for all C^{α} atoms, whereas the N- and C-terminal regions of the peptides are not superimposable. As described above, there are several similarities in the mode of interaction of the common residues pSer, Pro(+1), and Phe(+3) with the BRCT domains but also notable differences in the mode of interaction of residues at position +2. Previous crystal structures of these domains bound to phosphopeptides with a threonine[27,28,31,33] or a valine[30,32] residue at position +2 revealed how the side chains of these residues participated in the interaction. In the BRCT–ATRIP complex, the longer side chain of Gln(+2) is accommodated through a ~100° rotation of the E1698 side chain, as compared with the BRCT–BAAT1 structure (Figure 4A). The conformational change of E1698 may account, at least in part, for the lower affinity of the BRCA1 BRCTs for the ATRIP peptide.

Previous structural studies of the BRCT domains of BRCA1, MDC1,[41] and microcephalin (MCPH1)[42,43] bound to their cognate phosphopeptides revealed two crystallographic water molecules (corresponding to W1 and W2) at the interfaces of these complexes. Superposition of the BRCA1 BRCTs bound to the phosphopeptides ATRIP, BAAT1, BACH1, and CtIP with the MDC1 BRCT–γH2AX and MCPH1 BRCT–γH2AX complexes shows that these water molecules are conserved and form a hydrogen bonding network between BRCT and peptide residues (Figure 4B). In the BRCA1 structures, W1 participates in hydrogen bonding with the O^{3P} of pSer, the amide nitrogen of K1702, and W2, which hydrogen bonds with the carbonyl oxygen of Pro(+1) and the amide nitrogen of L1701 (Figures 2C and

dx.doi.org/10.1021/bi400714v | *Biochemistry* 2013, 52, 7618–7627

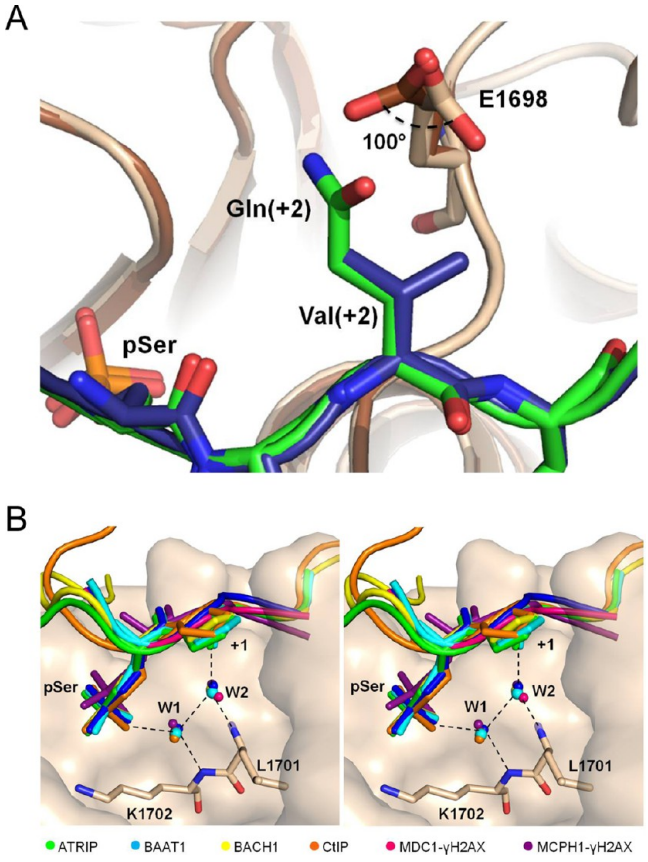

Figure 4. (A) Conformational change of the E1698 side chain in the BRCA1−ATRIP complex. Superposition of the crystal structures of the BRCA1 BRCTs (wheat) bound to ATRIP peptide (green) and the BRCTs (brown) bound to BAAT1 (blue) complexes. A dashed arc indicates the rotation of the E1698 side chain. (B) Stereoview of superposition of the BRCA1 BRCT complexes with ATRIP, BAAT1, BACH1 (PDB entry 1T15), CtIP (PDB entry 1Y98), the MDC1 BRCTs bound to γH2AX (PDB entry 2AZM), and the MCPH1 BRCTs complexed with γH2AX (PDB entry 3U3Z). The structurally conserved water molecules W1 and W2 that mediate the BRCT−peptide interaction are shown.

3C). In the MDC1 complex, W1 hydrogen bonds with the O^{1P} of pSer, W2, and the amide nitrogen of K1936, whereas W2 forms hydrogen bonds with the carbonyl oxygen of Gln(+1) and the amide nitrogen of V1935.[41] In the MCPH1−γH2AX complex, W1 hydrogen bonds with the O^{3P} of pSer, W2, and the amide nitrogen of N696, whereas W2 forms hydrogen bonds with the carbonyl oxygen of Gln(+1) and the amide nitrogen of L695.[42] Since these water molecules hydrogen bond with an O^{P} atom of pSer (an obligatory feature of the phosphopeptides recognized by the BRCA1, MDC1, and MCPH1 BRCT domains) and with main chain atoms of the BRCTs and peptide ligands, their arrangement is independent of the BRCT and peptide sequences. In fact, these water molecules are also observed in the crystal structures of the BRCT domains of TopBP1,[44] Rtt107,[45] and BARD1[46] (data not shown), and therefore appear to constitute an integral component of the BRCT recognition interface.

BRCA1 BRCT Recognition Motif. The plethora of BRCA1 BRCT binding partners[3−5] poses a challenge for the elucidation of the molecular mechanisms governing the hierarchy of target selection by these domains. Initial studies recognized the critical contribution of the two anchoring residues pSer and Phe(+3) in the binding affinity and derived the generally accepted recognition motif pS-X-X-F.[2,5,14,35] However, since all of the BRCA1 BRCT interaction partners contain these anchoring residues, the affinity and specificity of these interactions should be determined by amino acids surrounding these two residues, as was observed previously.[47] We therefore hypothesized that the residues at positions +1 and +2 might be responsible for the low affinity of the BRCA1 BRCTs for the BAAT1(pS156) and BAAT1(pS604) phosphopeptides. To explore the role of these residues in the BRCA1 BRCT−peptide interaction, we performed ITC experiments with variant BAAT1(pS156) and BAAT1(pS604) phosphopeptides that have Pro(+1) and Val(+2), residues that are present in the high-affinity peptides BAAT1(pS269) and CtIP.[30] As expected, replacement of Ser(+1) with Pro(+1) in the peptide BAAT1(pS156)S/P and of Leu(+2) with Val(+2) in BAAT1(pS156)L/V improved the binding of these peptides to BRCA1 BRCTs (Figure 5A and B), whereas substitution of both residues in the peptide BAAT1-(pS156)SL/PV resulted in stronger binding with a K_d of 30 μM (Figure 5C). Modeling of the peptide BAAT1(pS156) on the BRCA1 BRCT structure shows that the side chain of Ser(+1) likely abolishes the van der Waals contacts that are observed between N1774 and the C^{β} and C^{γ} atoms of Pro(+1) (Figures 2C and 5D). In addition, Pro(+1) likely contributes to the binding affinity by affecting the conformation of the peptide. Although Leu(+2) seems to be accommodated in the binding pocket at a distance of ∼2.6 Å from E1698 (Figure 5D), it is likely that the isobutyl group of Leu(+2) imposes a larger steric strain compared to the shorter isopropyl group of Val(+2).

In a similar series of experiments, substitution of Glu(+1) with Pro(+1) in the peptide BAAT1(pS604)E/P improved the binding (Figure 5E). Likewise, replacement of Gly(+2) with Val(+2) in the peptide BAAT1(pS604)G/V also increased the binding affinity (Figure 5F), whereas the substitution of both residues in BAAT1(pS604)EG/PV resulted in strong binding with an estimated K_d of 4.9 μM (Figure 5G). Modeling of the peptide BAAT1(pS604) on the BRCA1 BRCT structure shows a steric clash between Glu(+1) and N1774 (Figure 5H), whereas the lack of a side chain in Gly(+2) abolishes the van der Waals contacts between the $C^{\gamma 2}$ of Val(+2) and E1698 (Figures 3C and 5H), providing a possible structural explanation for the lower affinity of BAAT1(pS604) as compared to that of the mutated peptides. Notably, although the peptides BAAT(pS156)SL/PV and BAAT(pS604)EG/PV share an identical core sequence (DpSPVF), their affinities for the BRCA1 BRCTs differ by ∼6-fold (Figure 5C and G), indicating that residues outside the common sequence contribute significantly to the binding affinity. Taken together, these results demonstrate that the failure of the BRCA1 BRCTs to interact strongly with the BAAT1(pS156) and BAAT1(pS604) phosphopeptides is due mainly to the side chains at positions +1 and +2, with residues outside the motif pS-X-X-F also playing a role in the affinity of the interaction.

To further explore the contribution of the size and charge of the side chains at +1 and +2 in the binding affinity, we performed ITC experiments with the phosphopeptide CDC27(pS820) having the sequence HAAEpSDEF that corresponds to residues 816−823 of human CDC27 (cell division cycle 27), a component of the anaphase-promoting complex (GenBank entry AAA60471). Strikingly, the BRCA1 BRCTs did not interact with CDC27(pS820) despite the presence of the pS-X-X-F motif (Figure 6A). However, replacement of Asp(+1) with Pro(+1) in the peptide CDC27(pS820)D/P resulted in binding with an apparent K_d of 50.5 μM (Figure 6B), whereas

dx.doi.org/10.1021/bi400714v | Biochemistry 2013, 52, 7618−7627

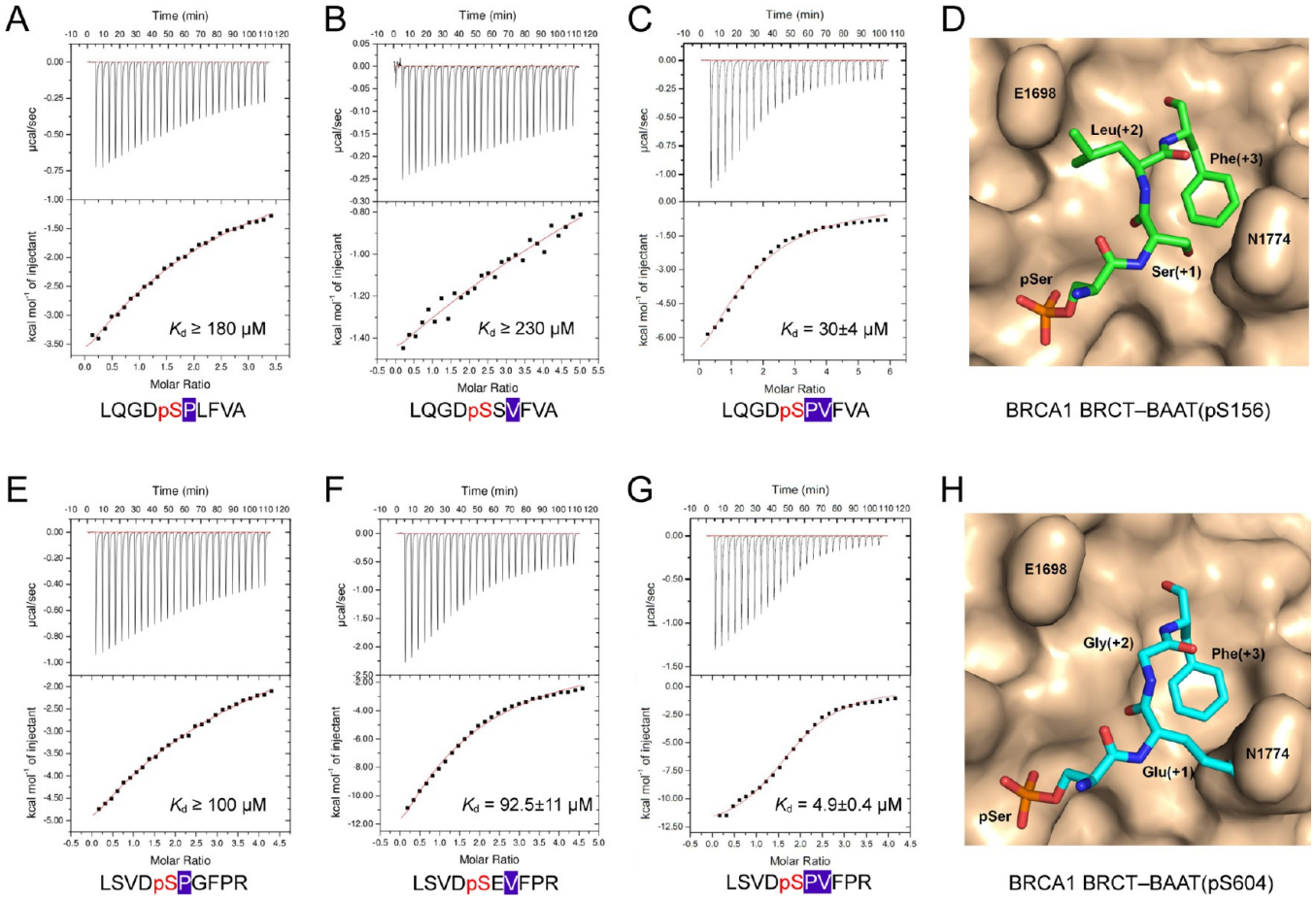

Figure 5. (A to C) Representative ITC results obtained for the BRCA1 BRCT interaction with the phosphopeptides BAAT(pS156)S/P, BAAT(pS156)L/V, and BAAT(pS156)SL/PV, respectively. The sequences of the peptides with phosphoserine (red) and the substituted residues (white letters on blue background) are shown at the bottom. For the isotherms in panels A–C, the BRCA1 BRCT concentration was 44.0 μM, 56.7 μM, and 22.7 μM, whereas the peptide concentration was 0.728 mM, 0.753 mM, and 0.676 mM, respectively. (D) Surface model of the BRCA1 BRCTs bound to the BAAT(pS156) peptide. (E to G) ITC results obtained for the BRCA1 BRCT interaction with the phosphopeptides BAAT(pS604)E/P, BAAT(pS604)G/V, and BAAT(pS604)EG/PV, respectively. The sequences of the peptides are shown at the bottom. For the isotherms in panels E–G, the BRCA1 BRCT concentration was 33.3 μM, 33.3 μM, and 18.9 μM, whereas the peptide concentration was 0.694 mM, 0.74 mM, and 0.413 mM, respectively. (H) Surface model of the BRCA1 BRCTs bound to the BAAT(pS604) peptide.

substitution of Glu(+2) with Thr(+2) in CDC27(pS820)E/T promoted strong binding with a K_d of 0.73 μM (Figure 6C). The ~69-fold higher affinity of CDC27(pS820)E/T compared to CDC27(pS820)D/P indicates that Glu(+2) has a more detrimental effect on the binding affinity than Asp(+1). Moreover, simultaneous substitutions of both acidic residues in the peptide CDC27(pS820)DE/PT restored very strong binding to the BRCTs with a K_d of 0.14 μM (Figure 6D). The extremely tight binding of the BRCA1 BRCTs to CDC27(pS820)DE/PT compared to that of other peptides harboring an internal pSPTF motif is likely due to recognition of the peptide C terminus, as has been shown previously.[33,43] Notably, the BRCA1 BRCT interaction with CDC27(pS820)D/P and CDC27(pS820)E/T produced biphasic thermograms composed of an initial exothermic component followed by an endothermic one (Figure 6B and C), whereas the CDC27(pS820)DE/PT generated an exothermic thermogram (Figure 6D). Although the obtained binding profiles were not studied further in the present work, these and similar peptides may be useful tools for the investigation of the driving forces, potential conformational changes during the BRCT–phosphopeptide interaction, and the order of the pSer and Phe(+3) insertion into the BRCT P_1 and P_2 pockets, respectively. It will therefore be important to determine in future studies whether the observed biphasic interaction profiles could be accounted for by models that involve two binding sites and determine the thermodynamic and structural mechanisms underlying the observed exothermic-to-endothermic transitions. Taken together, these results indicate that Glu(+2) is not favored by the BRCA1 BRCTs, whereas the concomitant presence of Asp(+1) and Glu(+2) adversely affects the affinity of these domains for the peptide.

To obtain structural insight into the BRCA1 BRCT selection against Glu(+2), we compared the BRCA1–ATRIP, MDC1–γH2AX,[41] and MCPH1–Cdc27[43] structures. The R1932 in MDC1 generates a basic region that favors acidic side chains at position +2 (Figure 6E). The corresponding area of MCPH1 (occupied by L692) also generates a positive electrostatic potential that accommodates the Glu(+2) of Cdc27 (Figure 6F). By contrast, BRCA1 has E1698 at the equivalent position, which creates an electrostatic repulsion with acidic side chains at position +2 (Figure 6G). Steric hindrance with E1698 may also contribute to lowering the affinity, as described for the side chain of Gln(+2). It is likely that accommodation of acidic and perhaps other unfavorable side chains at positions +1 and +2

dx.doi.org/10.1021/bi400714v | *Biochemistry* 2013, 52, 7618–7627

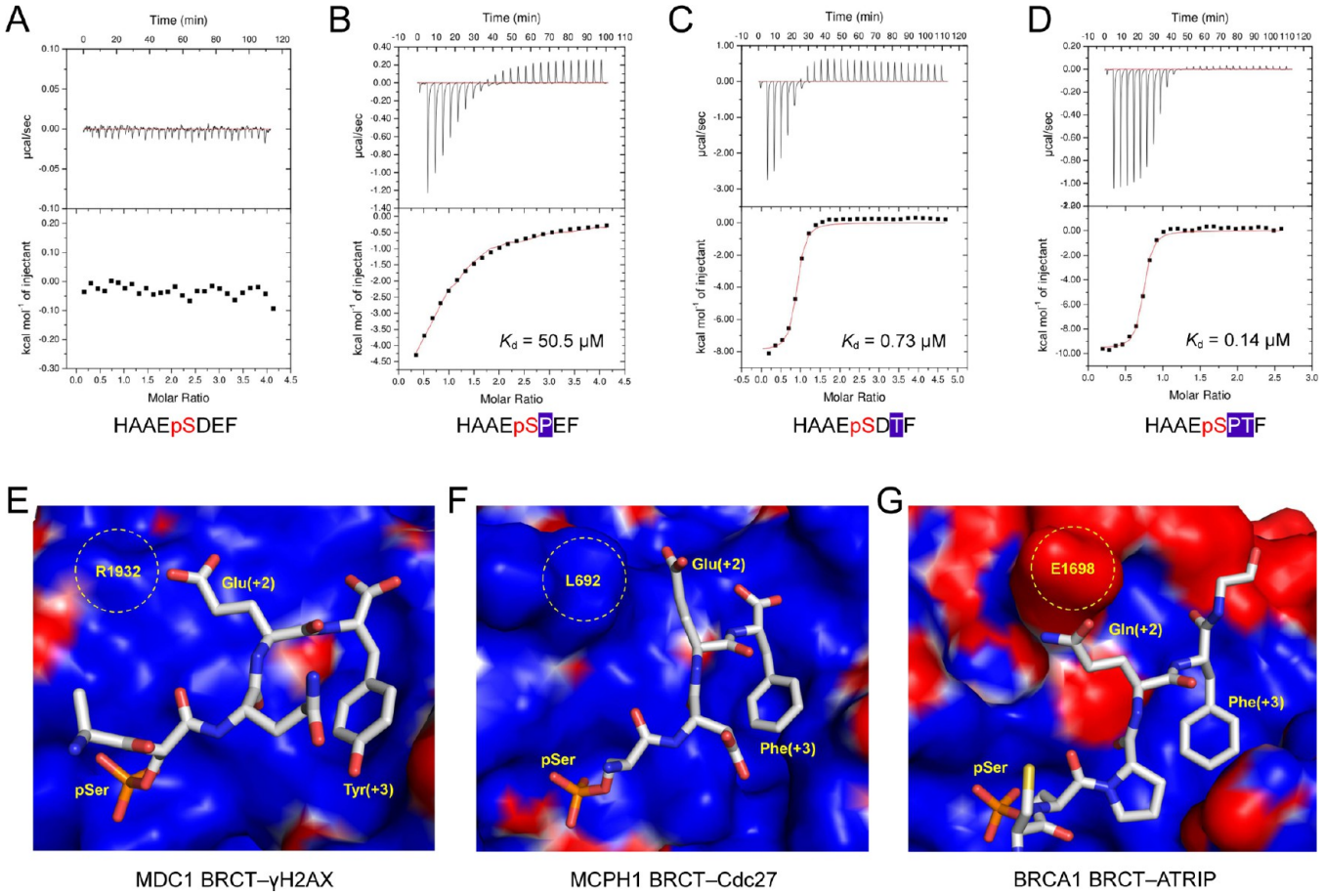

Figure 6. (A to D) ITC results obtained for the BRCA1 BRCT interaction with the phosphopeptides CDC27(pS820), CDC27(pS820)D/P, CDC27(pS820)E/T, and CDC27(pS820)DE/PT, respectively. For the isotherms in panels A–D, the BRCA1 BRCT concentration was 56.7 μM, 56.7 μM, 56.7 μM, and 29.5 μM, whereas the peptide concentration was 1.13 mM, 1.5 mM, 1.39 mM, and 0.369 mM, respectively. (E to G) Surface electrostatic potential of the MDC1, MCPH1, and BRCA1 BRCTs complexed with γH2AX, Cdc27, and ATRIP peptides (white stick models), respectively. The MDC1 R1932, MCPH1 L692, and BRCA1 E1698 residues that participate in the selection of Glu(+2) are labeled and encircled. Electrostatic potentials were calculated with PyMol and are colored red (acidic, -1 k_BT), white (neutral, 0 k_BT), and blue (basic, 1 k_BT).

depends on the number and strength of interactions between residues flanking the pS-X-X-F motif and BRCT residues. Nevertheless, it appears that the presence of Asp(+1)/Glu(+2) in CDC27 is sufficient to exclude the BRCA1 protein from the CDC27-mediated signaling pathways. Clearly, further studies are warranted to delineate the structural determinants underlying the complex recognition of phosphopeptides by these domains.

■ CONCLUDING REMARKS

The crystal structures of the BRCA1 BRCT domains bound to phosphopeptides ATRIP and BAAT1 elucidated the molecular determinants of their interaction and provided a structural basis for the BRCA1 function in ATRIP–ATR and BAAT1–ATM signaling, respectively. Notably, the BRCT–ATRIP structure revealed for the first time the mode of BRCA1 BRCT interaction with a phosphopeptide having Gln(+2) since to date, only structures of these domains bound to phosphopeptides having Thr(+2) or Val(+2) have been reported. Importantly, in the process of mapping the BRCA1 binding site on the BAAT1 protein we observed that certain side chains at positions +1 and +2 of the generally accepted BRCA1 BRCT recognition motif pS-X-X-F had detrimental effects on the affinity of the interaction. In particular, the combination of Asp(+1) and Glu(+2) in the peptide CDC27(pS820) adversely affected its interaction with the BRCA1 BRCTs. On the basis of these findings, we suggest that certain residues at these positions may impose severe electrostatic and/or steric constraints on the interaction with these domains. It is therefore imperative that the roles of the residues at positions +1 and +2 of the recognition motif pS-X-X-F, as well as those flanking this sequence, be systematically assessed and their contribution to the affinity and specificity of the interaction accurately determined in order to obtain a comprehensive understanding of the molecular mechanisms controlling the hierarchy of target selection by the BRCA1 BRCT domains during DDR and breast/ovarian oncogenesis. Knowledge of these mechanisms will also facilitate the structure-based design of specific inhibitors of BRCA1 BRCT binding to physiologic targets, with potential applications in cancer treatment through modulation of the DNA repair pathways.[48,49]

■ ASSOCIATED CONTENT

Accession Codes

PDB entry 4IGK (BRCA1–ATRIP complex) and PDB entry 4IFI (BRCA1–BAAT1 complex).

dx.doi.org/10.1021/bi400714v | *Biochemistry* 2013, 52, 7618–7627

AUTHOR INFORMATION

Corresponding Author

*Tel: 617-667-0064. E-mail: johnladias@gmail.com.

Funding

This work was supported by grant DA030209 from the National Institutes of Health, and grants W81XWH1010043, W81XWH1010602, W81XWH1110076, and W81XWH1110180 from the US Department of Defense to J.A.A.L.

Notes

The authors declare no competing financial interest.

ACKNOWLEDGMENTS

We thank the staff at the APS NE-CAT and NSLS X25 beamlines for assistance during data collection, and Dr. Olivier Kocher at Harvard Medical School for providing access to the microcalorimeter facility.

ABBREVIATIONS

ATM, ataxia telangiectasia mutated; ATR, ataxia telangiectasia and Rad3 related; ATRIP, ATR-interacting protein; BAAT1, BRCA1-associated protein required for ATM activation-1; BACH1, BRCA1-associated C-terminal helicase; BRCA1, breast and ovarian cancer susceptibility gene 1; BRCT, BRCA1 C-terminal; CDC27, cell division cycle 27; CtIP, CtBP-interacting protein; DDR, DNA damage response; DSB, DNA double-strand break; GST, glutathione *S*-transferase; ITC, isothermal titration calorimetry; MCPH1, microcephalin; MDC1, mediator of DNA damage checkpoint 1; MRN, Mre11−Rad50−Nbs1; PDB, Protein Data Bank; RPA, replication protein A; ssDNA, single-stranded DNA

REFERENCES

(1) Narod, S. A., and Foulkes, W. D. (2004) BRCA1 and BRCA2: 1994 and beyond. *Nat. Rev. Cancer 4*, 665−676.

(2) Venkitaraman, A. R. (2009) Linking the cellular functions of BRCA genes to cancer pathogenesis and treatment. *Annu. Rev. Pathol. 4*, 461−487.

(3) Roy, R., Chun, J., and Powell, S. N. (2011) BRCA1 and BRCA2: different roles in a common pathway of genome protection. *Nat. Rev. Cancer 12*, 68−78.

(4) Huen, M. S., Sy, S. M., and Chen, J. (2010) BRCA1 and its toolbox for the maintenance of genome integrity. *Nat. Rev. Mol. Cell Biol. 11*, 138−148.

(5) Caestecker, K. W., and Van de Walle, G. R. (2013) The role of BRCA1 in DNA double-strand repair: Past and present. *Exp. Cell Res. 319*, 575−587.

(6) Harper, J. W., and Elledge, S. J. (2007) The DNA damage response: ten years after. *Mol. Cell 28*, 739−745.

(7) Thompson, L. H. (2012) Recognition, signaling, and repair of DNA double-strand breaks produced by ionizing radiation in mammalian cells: the molecular choreography. *Mutat. Res. 751*, 158−246.

(8) Manke, I. A., Lowery, D. M., Nguyen, A., and Yaffe, M. B. (2003) BRCT repeats as phosphopeptide-binding modules involved in protein targeting. *Science 302*, 636−639.

(9) Yu, X., Chini, C. C., He, M., Mer, G., and Chen, J. (2003) The BRCT domain is a phospho-protein binding domain. *Science 302*, 639−642.

(10) Leung, C. C., and Glover, J. N. M. (2011) BRCT domains: easy as one, two, three. *Cell Cycle 10*, 2461−2470.

(11) Wang, B. (2012) BRCA1 tumor suppressor network: focusing on its tail. *Cell Biosci. 2*, 6.

(12) Li, M. L., and Greenberg, R. A. (2012) Links between genome integrity and BRCA1 tumor suppression. *Trends Biochem. Sci. 37*, 418−424.

(13) Silver, D. P., and Livingston, D. M. (2012) Mechanisms of BRCA1 tumor suppression. *Cancer Discovery 2*, 679−684.

(14) di Masi, A., Gullotta, F., Cappadonna, V., Leboffe, L., and Ascenzi, P. (2011) Cancer predisposing mutations in BRCT domains. *IUBMB Life 63*, 503−512.

(15) Shakya, R., Reid, L. J., Reczek, C. R., Cole, F., Egli, D., Lin, C. S., deRooij, D. G., Hirsch, S., Ravi, K., Hicks, J. B., Szabolcs, M., Jasin, M., Baer, R., and Ludwig, T. (2011) BRCA1 tumor suppression depends on BRCT phosphoprotein binding, but not its E3 ligase activity. *Science 334*, 525−528.

(16) Drost, R., Bouwman, P., Rottenberg, S., Boon, U., Schut, E., Klarenbeek, S., Klijn, C., van der Heijden, I., van der Gulden, H., Wientjens, E., Pieterse, M., Catteau, A., Green, P., Solomon, E., Morris, J. R., and Jonkers, J. (2011) BRCA1 RING function is essential for tumor suppression but dispensable for therapy resistance. *Cancer Cell 20*, 797−809.

(17) Derheimer, F. A., and Kastan, M. B. (2010) Multiple roles of ATM in monitoring and maintaining DNA integrity. *FEBS Lett. 584*, 3675−3681.

(18) Ditch, S., and Paull, T. T. (2012) The ATM protein kinase and cellular redox signaling: beyond the DNA damage response. *Trends Biochem. Sci. 37*, 15−22.

(19) McKinnon, P. J. (2012) ATM and the molecular pathogenesis of ataxia telangiectasia. *Annu. Rev. Pathol. 7*, 303−321.

(20) Flynn, R. L., and Zou, L. (2011) ATR: a master conductor of cellular responses to DNA replication stress. *Trends Biochem. Sci. 36*, 133−140.

(21) Nam, E. A., and Cortez, D. (2011) ATR signalling: more than meeting at the fork. *Biochem. J. 436*, 527−536.

(22) Bunting, S. F., Callén, E., Kozak, M. L., Kim, J. M., Wong, N., López-Contreras, A. J., Ludwig, T., Baer, R., Faryabi, R. B., Malhowski, A., Chen, H. T., Fernandez-Capetillo, O., D'Andrea, A., and Nussenzweig, A. (2012) BRCA1 functions independently of homologous recombination in DNA interstrand crosslink repair. *Mol. Cell 46*, 125−135.

(23) Venere, M., Snyder, A., Zgheib, O., and Halazonetis, T. D. (2007) Phosphorylation of ATR-interacting protein on Ser239 mediates an interaction with breast-ovarian cancer susceptibility 1 and checkpoint function. *Cancer Res. 67*, 6100−6105.

(24) Aglipay, J. A., Martin, S. A., Tawara, H., Lee, S. W., and Ouchi, T. (2006) ATM activation by ionizing radiation requires BRCA1-associated BAAT1. *J. Biol. Chem. 281*, 9710−9718.

(25) Puffenberger, E. G., Jinks, R. N., Sougnez, C., Cibulskis, K., Willert, R. A., Achilly, N. P., Cassidy, R. P., Fiorentini, C. J., Heiken, K. F., Lawrence, J. J., Mahoney, M. H., Miller, C. J., Nair, D. T., Politi, K. A., Worcester, K. N., Setton, R. A., Dipiazza, R., Sherman, E. A., Eastman, J. T., Francklyn, C., Robey-Bond, S., Rider, N. L., Gabriel, S., Morton, D. H., and Strauss, K. A. (2012) Genetic mapping and exome sequencing identify variants associated with five novel diseases. *PLoS One 7*, e28936.

(26) Saunders, C. J., Miller, N. A., Soden, S. E., Dinwiddie, D. L., Noll, A., Alnadi, N. A., Andraws, N., Patterson, M. L., Krivohlavek, L. A., Fellis, J., Humphray, S., Saffrey, P., Kingsbury, Z., Weir, J. C., Betley, J., Grocock, R. J., Margulies, E. H., Farrow, E. G., Artman, M., Safina, N. P., Petrikin, J. E., Hall, K. P., and Kingsmore, S. F. (2012) Rapid whole-genome sequencing for genetic disease diagnosis in neonatal intensive care units. *Sci. Transl. Med. 4*, 154ra135.

(27) Clapperton, J. A., Manke, I. A., Lowery, D. M., Ho, T., Haire, L. F., Yaffe, M. B, and Smerdon, S. J. (2004) Structure and mechanism of BRCA1 BRCT domain recognition of phosphorylated BACH1 with implications for cancer. *Nat. Struct. Mol. Biol. 11*, 512−518.

(28) Shiozaki, E. N., Gu, L., Yan, N., and Shi, Y. (2004) Structure of the BRCT repeats of BRCA1 bound to a BACH1 phosphopeptide: implications for signaling. *Mol. Cell 14*, 405−412.

(29) Botuyan, M. V., Nomine, Y., Yu, X., Juranic, N., Macura, S., Chen, J., and Mer, G. (2004) Structural basis of BACH1 phosphopeptide

recognition by BRCA1 tandem BRCT domains. *Structure 12*, 1137−1146.
(30) Varma, A. K., Brown, R. S., Birrane, G., and Ladias, J. A. A. (2005) Structural basis for cell cycle checkpoint control by the BRCA1−CtIP complex. *Biochemistry 44*, 10941−10946.
(31) Shen, Y., and Tong, L. (2008) Structural evidence for direct interactions between the BRCT domains of human BRCA1 and a phospho-peptide from human ACC1. *Biochemistry 47*, 5767−5773.
(32) Williams, R. S., Lee, M. S., Hau, D. D., and Glover, J. N. M. (2004) Structural basis of phosphopeptide recognition by the BRCT domain of BRCA1. *Nat. Struct. Mol. Biol. 11*, 519−525.
(33) Campbell, S. J., Edwards, R. A., and Glover, J. N. M. (2010) Comparison of the structures and peptide binding specificities of the BRCT domains of MDC1 and BRCA1. *Structure 18*, 167−176.
(34) Tischkowitz, M., Hamel, N., Carvalho, M. A., Birrane, G., Soni, A., van Beers, E. H., Joosse, S. A., Wong, N., Novak, D., Quenneville, L. A., Grist, S. A., kConFab, Nederlof, P. M., Goldgar, D. E., Tavtigian, S. V., Monteiro, A. N., Ladias, J. A. A., and Foulkes, W. D. (2008) Pathogenicity of the BRCA1 missense variant M1775K is determined by the disruption of the BRCT phosphopeptide-binding pocket: a multimodal approach. *Eur. J. Hum. Genet. 16*, 820−832.
(35) Coquelle, N., Green, R., and Glover, J. N. M. (2011) Impact of BRCA1 BRCT domain missense substitutions on phosphopeptide recognition. *Biochemistry 50*, 4579−4589.
(36) Otwinowski, Z., and Minor, W. (1997) Processing of X-ray diffraction data collected in oscillation mode. *Methods Enzymol. 276*, 307−326.
(37) McCoy, A. J., Grosse-Kunstleve, R. W., Adams, P. D., Winn, M. D., Storoni, L. C., and Read, R. J. (2007) Phaser crystallographic software. *J. Appl. Crystallogr. 40*, 658−674.
(38) Murshudov, G. N., Skubák, P., Lebedev, A. A., Pannu, N. S., Steiner, R. A., Nicholls, R. A., Winn, M. D., Long, F., and Vagin, A. A. (2011) REFMAC5 for the refinement of macromolecular crystal structures. *Acta Crystallogr., Sect. D 67*, 355−367.
(39) Winn, M. D., Ballard, C. C., Cowtan, K. D., Dodson, E. J., Emsley, P., Evans, P. R., Keegan, R. M., Krissinel, E. B., Leslie, A. G., McCoy, A., McNicholas, S. J., Murshudov, G. N., Pannu, N. S., Potterton, E. A., Powell, H. R., Read, R. J., Vagin, A., and Wilson, K. S. (2011) Overview of the CCP4 suite and current developments. *Acta Crystallogr., Sect. D 67*, 235−242.
(40) Emsley, P., and Cowtan, K. (2004) Coot: model-building tools for molecular graphics. *Acta Crystallogr., Sect. D 60*, 2126−2132.
(41) Stucki, M., Clapperton, J. A., Mohammad, D., Yaffe, M. B., Smerdon, S. J., and Jackson, S. P. (2005) MDC1 directly binds phosphorylated histone H2AX to regulate cellular responses to DNA double-strand breaks. *Cell 123*, 1213−1226.
(42) Singh, N., Basnet, H., Wiltshire, T. D., Mohammad, D. H., Thompson, J. R., Héroux, A., Botuyan, M. V., Yaffe, M. B., Couch, F. J., Rosenfeld, M. G., and Mer, G. (2012) Dual recognition of phosphoserine and phosphotyrosine in histone variant H2A.X by DNA damage response protein MCPH1. *Proc. Natl. Acad. Sci. U.S.A. 109*, 14381−14386.
(43) Singh, N., Wiltshire, T. D., Thompson, J. R., Mer, G., and Couch, F. J. (2012) Molecular basis for the association of microcephalin (MCPH1) protein with the cell division cycle protein 27 (Cdc27) subunit of the anaphase-promoting complex. *J. Biol. Chem. 287*, 2854−2862.
(44) Leung, C. C., Gong, Z., Chen, J., and Glover, J. N. M. (2011) Molecular basis of BACH1/FANCJ recognition by TopBP1 in DNA replication checkpoint control. *J. Biol. Chem. 286*, 4292−4301.
(45) Li, X., Liu, K., Li, F., Wang, J., Huang, H., Wu, J., and Shi, Y. (2012) Structure of C-terminal tandem BRCT repeats of Rtt107 protein reveals critical role in interaction with phosphorylated histone H2A during DNA damage repair. *J. Biol. Chem. 287*, 9137−9146.
(46) Birrane, G., Varma, A. K., Soni, A., and Ladias, J. A. A. (2007) Crystal structure of the BARD1 BRCT domains. *Biochemistry 46*, 7706−7712.
(47) Yuan, Z., Kumar, E. A., Kizhake, S., and Natarajan, A. (2011) Structure-activity relationship studies to probe the phosphoprotein binding site on the carboxy terminal domains of the breast cancer susceptibility gene 1. *J. Med. Chem. 54*, 4264−4268.
(48) Yuan, Z., Kumar, E. A., Campbell, S. J., Palermo, N. Y., Kizhake, S., Glover, J. N. M., and Natarajan, A. (2011) Exploiting the P-1 pocket of BRCT domains toward a structure guided inhibitor design. *ACS Med. Chem. Lett. 2*, 764−767.
(49) Pessetto, Z. Y., Yan, Y., Bessho, T., and Natarajan, A. (2012) Inhibition of BRCT(BRCA1)-phosphoprotein interaction enhances the cytotoxic effect of olaparib in breast cancer cells: a proof of concept study for synthetic lethal therapeutic option. *Breast Cancer Res Treat. 134*, 511−517.
(50) Laskowski, R. A., and Swindells, M. B. (2011) LigPlot+: multiple ligand-protein interaction diagrams for drug discovery. *J. Chem. Inf. Model. 51*, 2778−2786.